Electronic Supplementary Information

A Promising Bulky Anion Based Lithium Borate Salt for Lithium Metal Batteries

Lixin Qiao,[ab] Zili Cui,*[b] Bingbing Chen,[b] Gaojie Xu,[b] Zhonghua Zhang,[b] Jun Ma,[b] Huiping Du,[b] Xiaochen Liu,[b] Suqi Huang,[c] Kun Tang,[ab] Shanmu Dong,[b] Xinhong Zhou,*[a] Guanglei Cui*[b]

[a]College of Chemistry and Molecular Engineering, Qingdao University of Science & Technology, Qingdao, 266042, P. R. China.
*E-mail: zxhhx2008@163.com.

[b]Qingdao Industrial Energy Storage Research Institute, Qingdao Institute of Bioenergy and Bioprocess Technology, Chinese Academy of Sciences, Qingdao, 266101, P. R. China.

*E-mail: cuigl@qibebt.ac.cn; Tel.: 86-532-80662746; fax: 86-532-80662746.

[c]School of Chemistry and Chemical Engineering, Qingdao University, Qingdao, 266071, P. R. China.

1. Experimental method

1.1 Material

Perfluoro-tert-butylalcohol (Fluorochem), propylene carbonate (PC) (98%, Macklin), dimethyl carbonate (DMC) (98%, Macklin) and acetonitrile (99.5%, Sigma Aldrich) were used as received without any treating process. n-Butyllithium (1.6 M in hexane) and boron trifluoride diethyl etherate (98%) were bought from Sigma Aldrich and Macklin, respectively. Lithium bis(trifluoromethanesulfonimide) (LiTFSI) and $LiBF_4$ (99.99%) were purchased from Aladdin and retreated at 120 °C in vacuum oven for 12 hours. The tetrahydrofuran (THF) (AR, Sinopharm Chemical Reagent Limited Company) and 1,2-dimethoxyethane (DME) (99.5%, Sigma Aldrich) solvents were refluxed with sodium using benzophenone as indicator and distilled with 4 Å molecular sieve under Ar atmosphere. 1.0 M $LiBF_4$/PC and 1.0 M LiTFSI/PC were obtained by dissolving the stoichiometric $LiBF_4$ and LiTFSI in PC solvent, respectively. The 1.0 M LiTFPFB/PC electrolyte was prepared by the same method using the synthesized lithium salt in this work. All the electrolytes were prepared in the glove box with the content of O_2 and H_2O below 0.1 ppm.

1.2 Synthesis and characterization of LiTFPFB salt

The procedure for the synthesis of LiTFPFB salt is depicted in Scheme S1.

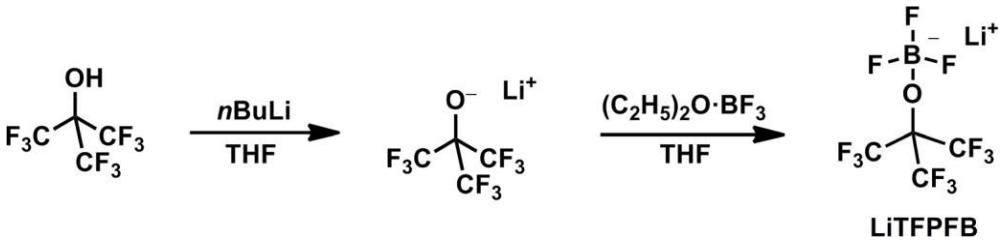

Scheme S1. The synthesis route of LiTFPFB salt.

1.2.1 Synthesis procedure of $Li[(CF_3)_3CO]$

Perfluoro-tert-butylalcohol (0.944g, 4 mmol) was added to 2 ml THF solvent under normal stirring conditions. Then 2.5 ml n-Butyllithium was added slowly under Ar atmosphere. After that THF solvent was removed on a rotary evaporators and a crude product was obtained. Subliming under vacuum afforded 0.72 g product (75%).

^{13}C NMR and ^{19}F NMR spectra of the product in DMSO-d_6 were conducted on a nuclear magnetic resonance spectrometer (Bruker AVANCE-III 400). The products were also characterized by Electrospray ionization mass spectrometry (ESI-MS) which was performed on a four-sector (BE/BE) tandem mass spectrometer (JMS-700T, JEOL) equipped with the ESI source.

NMR: δ (400 MHz, [ppm], DMSO-d_6): ^{13}C NMR (100.57 MHz), 125.69 (q, J = 298.0 Hz), 85.31 (m). ^{19}F (376.06 MHz), -75.13 (s). MS (ESI): m/z = 234.9323 was assigned to $[(CF_3)_3CO]^-$ in $Li[(CF_3)_3CO]$. The HR-MS and NMR spectra of $Li[(CF_3)_3CO]$ are depicted in Figure S1-2.

1.2.2 Synthesis procedure of LiTFPFB

In a glove box, Li[$(CF_3)_3CO$] (0.484 g, 2 mmol) was added to 2 ml THF solvent in a round-bottom flask and a transparent solution was obtained. Then the solution was added to 0.282 g boron trifluoride diethyl etherate dissolved in 2 ml THF dropwise under stirring conditions, and a colorless & transparent solution was gained. Thereafter, the solvent was volatilized under Argon atmosphere, and a white solid was obtained. Finally, the solid was washed with acetonitrile (3 ml × 3) three times. Drying under vacuum afforded 0.41 g product (66%). NMR: δ (400 MHz, [ppm], DMSO-d_6): ^{19}F (376.06 MHz), δ = -71.92 (q, J = 4.0 Hz, 9 F), -144.71 (m, 3F). ^{11}B (128.32), δ = -0.91 (q, J = 16.0 Hz). ^{7}Li NMR (s, 0.03). MS (ESI): m/z = 302.9860 was assigned to $[(CF_3)_3COBF_3]^-$ in LiTFPFB. The NMR and HR-MS spectra of LiTFPFB are depicted in Figure 1.

1.3 Electrochemical characterization

Ionic conductivities of the electrolytes with a PP2500 separator between two stainless steel plates were conducted by an AC impedance analysis using a BioLogic VMP-300 with an AC voltage amplitude of 10 mV over the frequency range from 1 Hz to 1 MHz. The ionic conductivity of these electrolytes were calculated by the following equation

$$\sigma = \quad — \qquad (1)$$

where L presents the thickness of separator, S is the contact area between

electrode and electrolyte, and R is the bulk resistance of the electrolyte. The interfacial compatibility of lithium metal with different electrolytes was assessed by the same instrument for the ionic conductivity measurement over a frequency range of 1 MHz-10 mHz using Li/electrolyte/Li cells.

In this paper, the Al passivation measurement was evaluated by chronoamperometry and cyclic voltammetry (scan rate was 1 mV s^{-1} from 2.5 V to 5.0 V) performed on a working electrode of fresh Al foil and a counter and reference electrode of lithium metal in a coin cell (CR2032-type). The Al foil was polished with a sandpaper and washed with DME three times in the glove box, followed by drying in the transition cabin for 1 hour. The oxidative stability of the LiTFPFB electrolytes was evaluated by linear sweep voltammetry using the platinum as the working electrode and metal lithium as the counter and reference electrodes at a scanning rate of 5 mV s^{-1}.

The Li ion transference number was determined by the potentiostatic polarization test on the Li/electrolyte/Li cell with a potential of 10 mV. The initial and steady impedance before and after polarization scan were determined by electrochemical impedance spectroscopy measurements.

$$t_{+} = \frac{I_{ss}(\Delta V - I_0 R_0^{ss})}{I_0(\Delta V - I_{ss} R_{ss})}$$

In which, t_{+} is the cationic transference number, ΔV is the potential applied to the cell, R_0^{ss} and R_{ss} are the initial and steady-state

resistances, I_0 and I_s are the initial and steady-state currents.

For cell test, the $LiFePO_4$ cathode was prepared via a traditional casting method, by mixing 80 wt% $LiFePO_4$, 10 wt% acetylene black, and 10 wt% LA133 as binder. Finally, the mass loading of the active material on the $LiFePO_4$ cathode was about 1.5 mg cm^{-2}. $LiCoO_2$ cathode mixing the 80 wt% $LiCoO_2$, 10 wt% acetylene black and 10 wt% PVDF (polyvinylidene fluoride) binder was also prepared by casting on Al foil. The active mass loading of the $LiCoO_2$ electrode was about 1.4 mg cm^{-2}. The theoretical capacity of the obtained $LiFePO_4$ and $LiCoO_2$ cathodes are approximately 160 and 140 mAh g^{-1}, respectively. All the cells were assembled in an argon-filled glove box (the content of H_2O and O_2 was less than 0.1 ppm). The galvanostatic charge/discharge test of $LiFePO_4$/Li coin cells between 2.5-4.0 V at varied current densities was conducted on LAND test system (Wuhan LAND electronics Co., Ltd.). The $LiCoO_2$/Li cells were charged and discharged between 2.75-4.35 V.

Cu/Li cells of the both electrolytes were charged/discharged for 1 h during each process at a constant current density of 0.5 mA cm^{-2} to evaluate the lithium deposition/dissolution efficiency. To investigate the cycle performance at room temperature, the $LiFePO_4$/Li or $LiCoO_2$/Li cells were cycled at 0.2 C for the first three cycles and at 1 C for the remaining cycles. The low temperature performances of $LiFePO_4$/Li cells were investigated at 0.2 C at -5 ℃. The cycle performance of $LiFePO_4$/Li

cells at 60 °C were measured at 1 C for the first three cycles and 5 C for the following cycles. The rate performance tests were conducted under various current densities of 0.2 C, 0.5 C, 1 C, 2 C, 3 C, 4 C, 5 C and 1 C at room temperature, and 0.2 C, 0.5 C, 1 C, 2 C, 4 C, 6 C, 8 C, 10 C and 4 C at 60 °C .

The impedance variation of $LiFePO_4$/Li cells using $LiBF_4$ and LiTFPFB electrolytes with cycling were investigated at room temperature. After 1^{st}, 50^{th}, 100^{th}, 200^{th} cycles, the impedance was tested on the BioLogic VMP-300 impedance instrument and the data was summarized in Table S1.

1.4 Characterization of the electrodes

The cycled cells were disassembled in argon glove-box with O_2 and H_2O content lower than 0.1 ppm. The obtained anodes were rinsed with dimethyl carbonate (DMC) to remove the residual lithium salts and solvents, and then dried in vacuum for 5 hours at room temperature. Surface morphology of the cycled electrodes was characterized by HITACHI (SU8010) field emission scanning electron microscope (FE-SEM). X-ray photoelectron spectroscopy (XPS) with Al Kα radiation was performed using a PHI 3056 XPS under ultrahigh vacuum conditions to analyze the surface chemical composition of the cycled electrodes. The C 1s binding energy at 284.6 eV was used as a reference to calibrate the energy scale.

1.5 DFT calculations

DFT calculations: All geometry optimizations were performed at the B3LYP /6-31G(p,d)* level in the gas phase. The PC solvent wasn't taken into account. All energy calculations were performed in solution using Gaussian 09 package.

2. Experiment results description

2.1 Identification of the effective species in LiTFPFB electrolyte

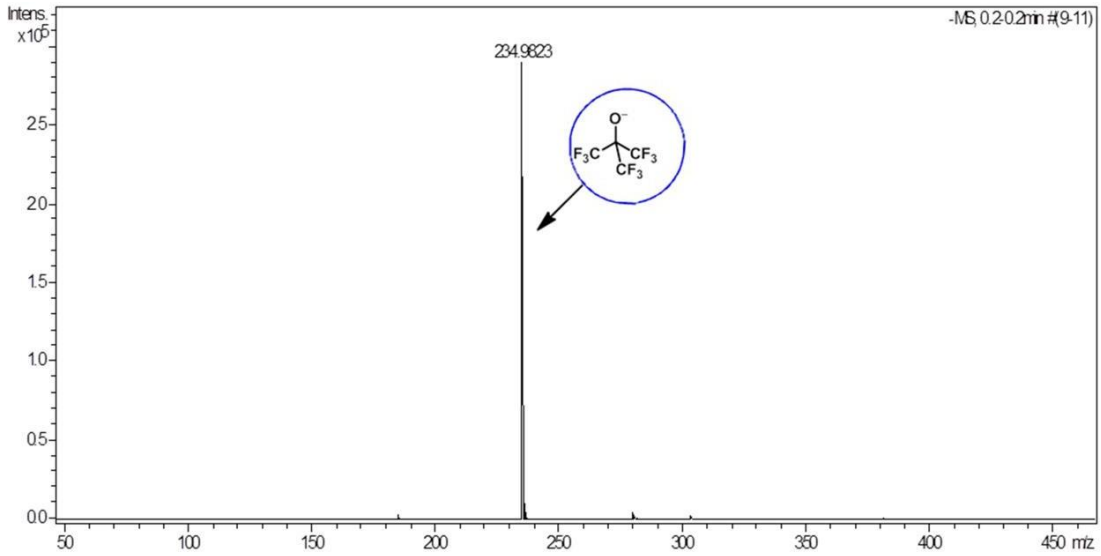

Figure S1. HR-MS of $Li[(CF_3)_3CO]$.

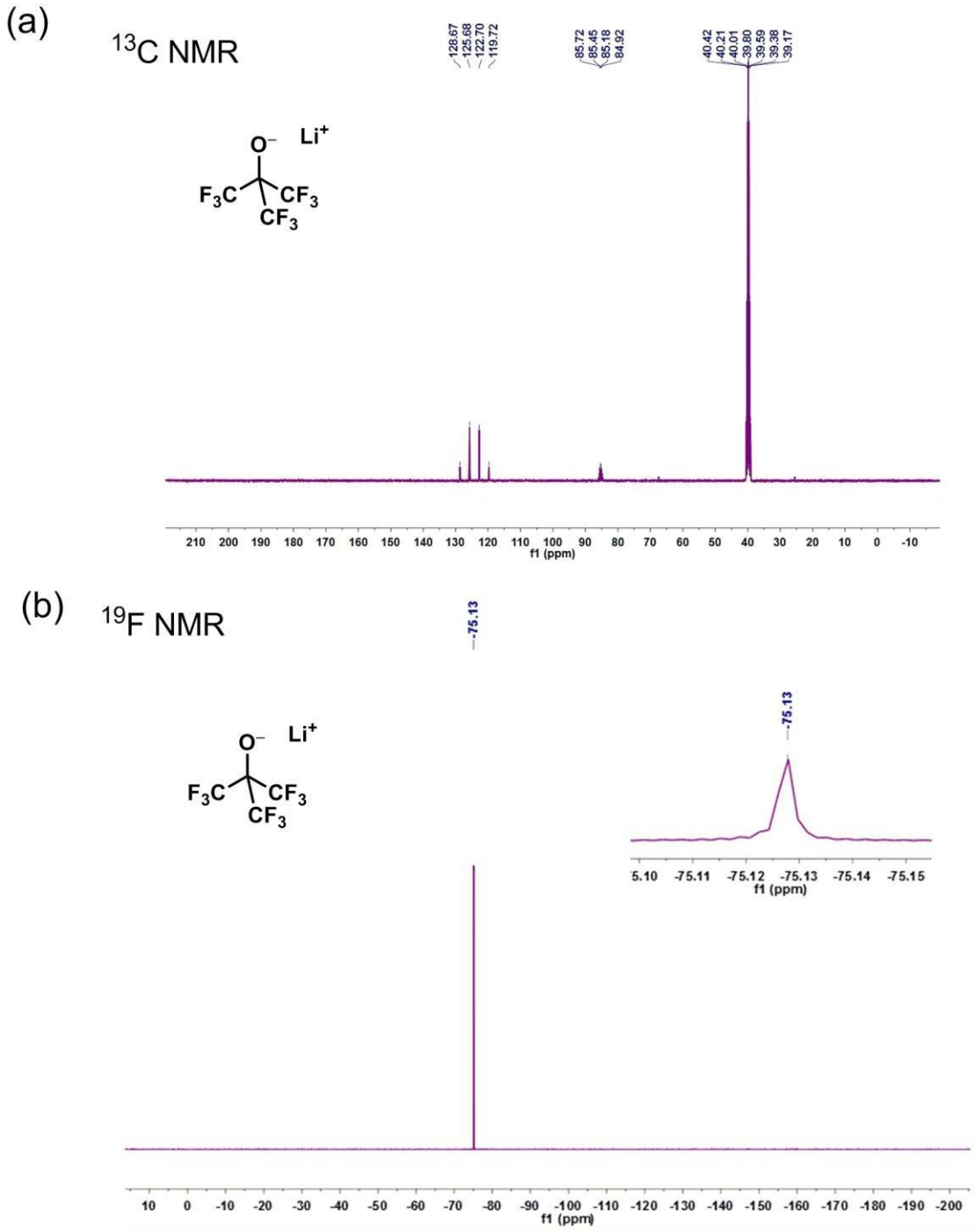

Figure S2. ^{13}C NMR (a) and ^{19}F NMR (b) spectra of $Li[(CF_3)_3CO]$.

2.2 Ion transference number of LiTFPFB salt in PC solvent

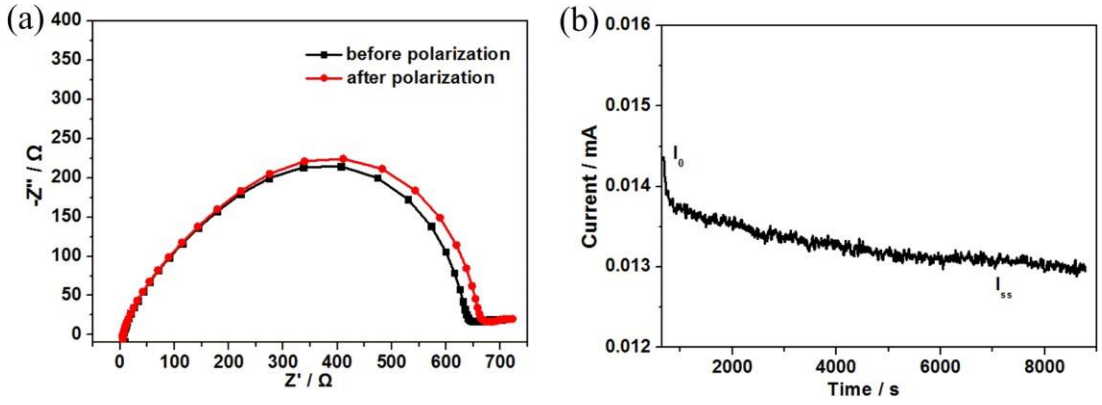

Figure S3. (a) Electrochemical impedance spectrum (EIS) for Li/LiTFPFB/Li cell before and after polarization. (b) Direct current (DC) polarization curve with the potential of 10 mV.

Li-ion transference number (t_{Li^+}) of the 1.0 M LiTFPFB electrolyte was 0.48 through DC polarization and EIS measurement.

2.3 The stability of the $LiBF_4$ electrolyte to the Al current

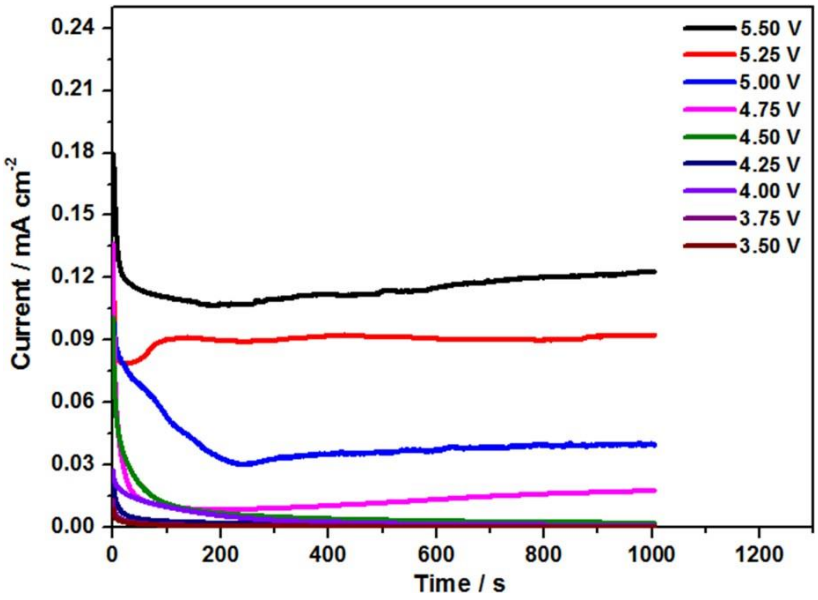

Figure S4. Time-decaying current density obtained on an Al electrode using 1.0 M $LiBF_4$/PC at varied potentials vs. Li^+/Li.

2.4 The interface stability of Li anode to electrolytes

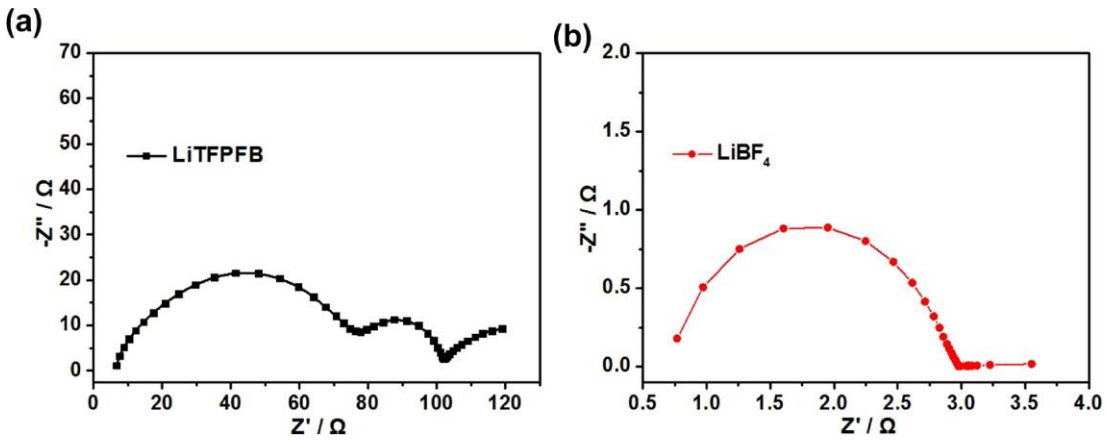

Figure S5. Nyquist plots of LiTFPFB and $LiBF_4$ based Li/Li symmetrical cells measured at open-circuit potential after 500-hour (a) and 480-hour (b) cycling, respectively.

As shown in Figure S5a, after 500 cycles, the R_b, R_{SEI}, and R_{ct} of the LiTFPFB based cell are 5 Ω, 75 Ω and 17 Ω, respectively, while the $LiBF_4$ based cell only shows an ohmic resistance of 3 Ω (Figure S5b), which indicates the $LiBF_4$ based cell is short circuit after 480-hour cycling.

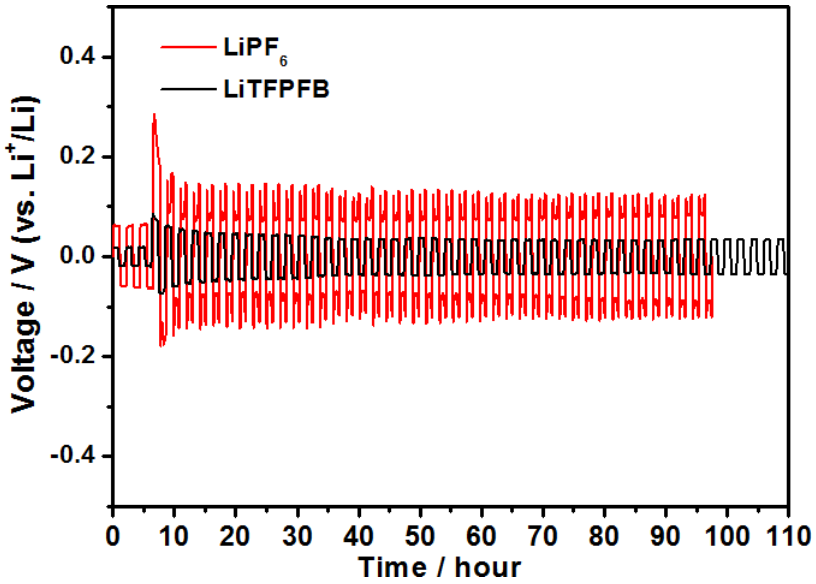

Figure S6. Lithium plating/stripping of LiTFPFB and $LiPF_6$ based Li/Li symmetrical cells at a current density of 0.5 mA cm^{-2}.

The polarization tests of the Li/Li symmetrical cells with LiTFPFB and $LiPF_6$ based electrolytes are performed to investigate the interfacial stability of the Li/electrolyte interface. The Li/Li symmetrical cells of both electrolytes are charged/discharged for 1 h during each process at a current density of 0.5 mA cm^{-2}. As shown in Figure S6, the $LiPF_6$ based cell shows a drastic fluctuation during each charge-discharge process with a higher overpotential of 0.15 V until 100 hours. In contrast, the plating/stripping of lithium occurs at a low overpotential below 0.1 V in the whole process, indicating that LiTFPFB plays a positive role in stabilizing the Li/electrolyte interface.

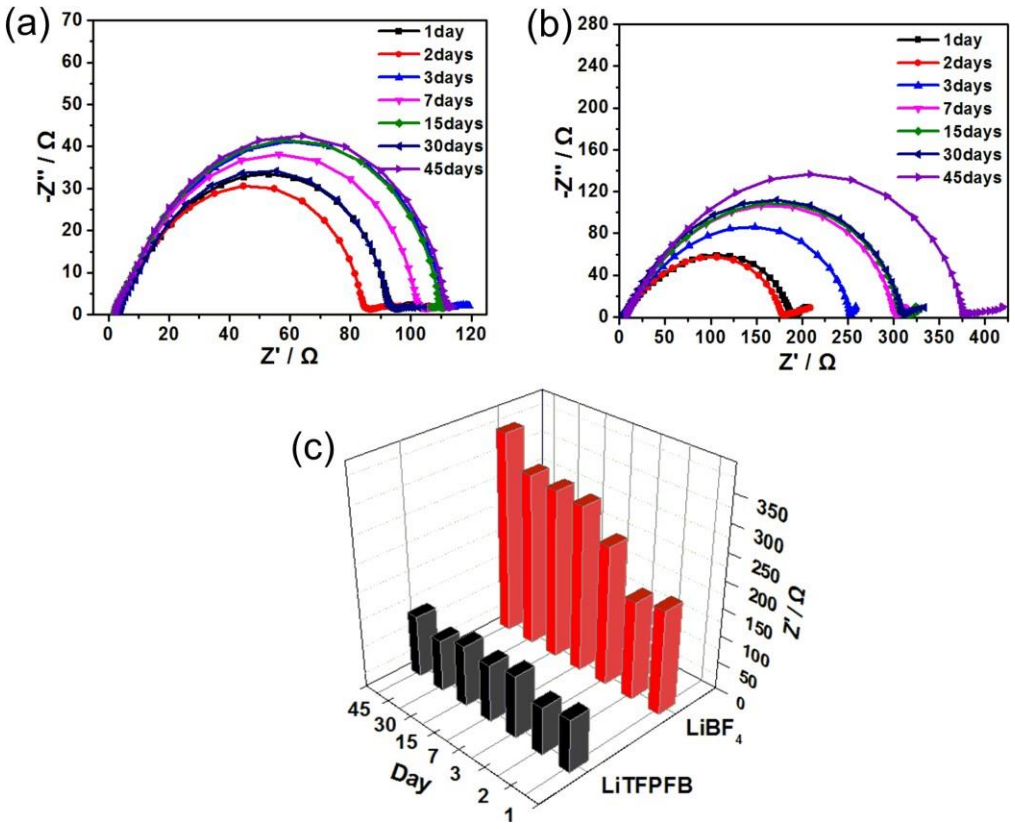

Figure S7. The AC-impedance evoluation of 1.0 M LiTFPFB (a) and 1.0 M $LiBF_4$ (b) electrolytes in Li/Li symmetric cells over time at room temperature. (c) Interfacial resistance evolution of 1.0 M LiTFPFB and 1.0 M $LiBF_4$ electrolytes in Li/Li symmetrical cells over time.

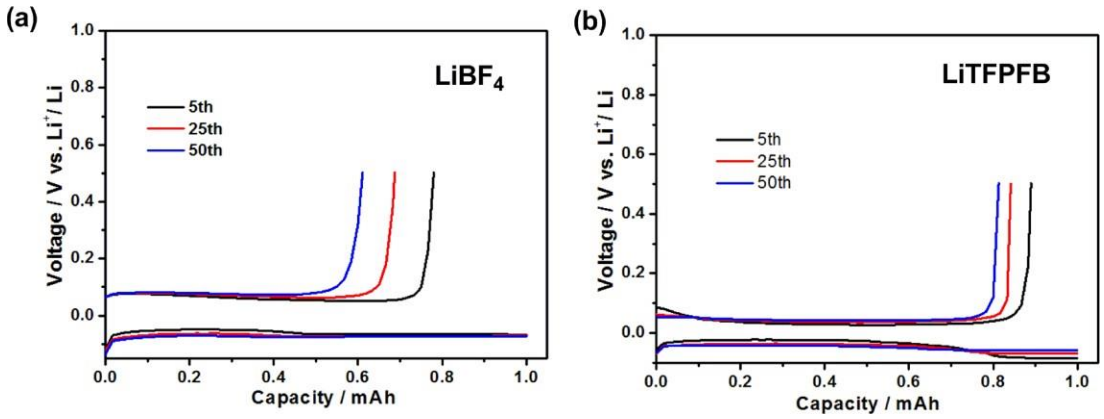

Figure S8. Electrochemical performance of Li metal plating/stripping on a Cu working electrode using 1.0 M $LiBF_4$/PC (a) and 1.0 M LiTFPFB/PC (b) electrolytes.

The coin-type Cu/Li cells with 1.0 M $LiBF_4$/PC and 1.0 M LiTFPFB/PC electrolytes were used to investigate the cycling stability of Li plating/striping. The Coulombic efficiency (CE) of the Li plating/striping can be calculated from the ratio of Li removed from Cu substrate to that deposited during the same cycle. Figure S8a and b compare the voltage profiles at different cycles using different electrolytes. For both electrolytes, although the charging behaviors remain the same over 50 cycles, less and less Li could be stripped from the Cu electrode with increasing cycles. This may mean that a considerable amount of Li deposited on the substrate reacted with the electrolyte and could not be covered during the stripping processes. It should be mentioned that the LiTFPFB based electrolyte shows higher stability with Li metal compared with $LiBF_4$ based one because the CE of the Li plating/stripping of the former is about 80.6% after 50 cycles, which is much higher than that of the latter (60.3%).

2.5 Room temperature performance of LiTFPFB

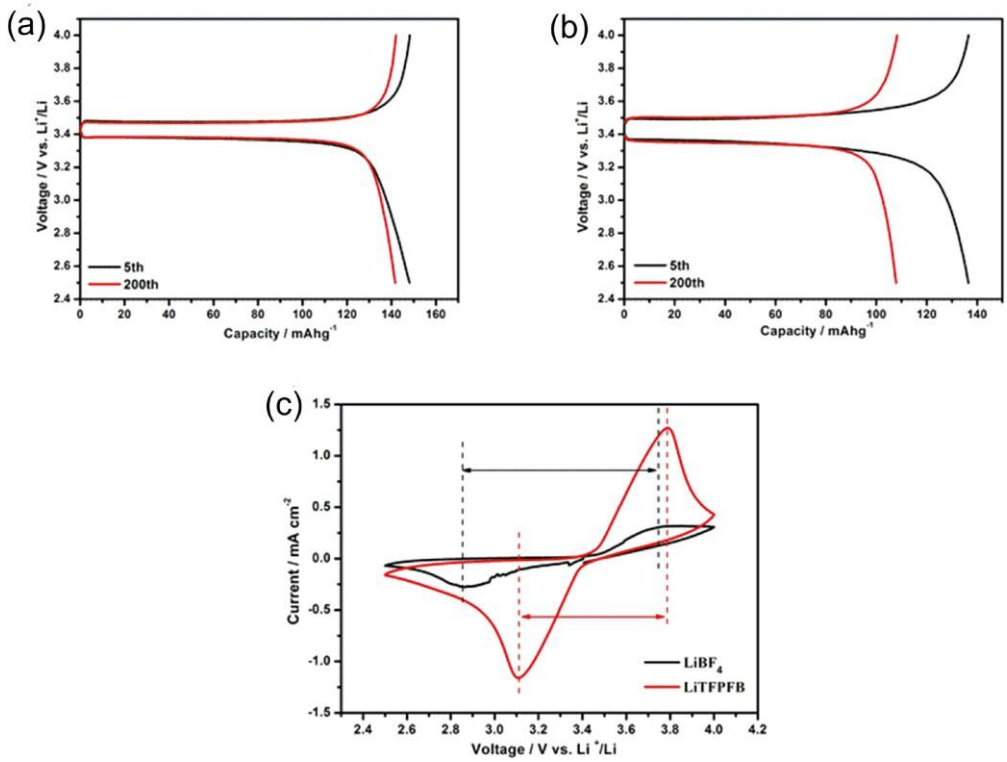

Figure S9. The charge/discharge curves of LiTFPFB (a) and $LiBF_4$ (b) based $LiFePO_4$/Li cells at 5^{th} and 200^{th} cycles. (c) CV curves for $LiFePO_4$/Li cells with 1.0 M LiTFPFB and 1.0 M $LiBF_4$ electrolytes after 200 cycles.

It can be seen from Figure S9a and S9b, after 5 cycles activation process, the LiTFPFB based battery shows a lower overpotential (0.10 V) compared with $LiBF_4$ based electrolyte (0.12 V). After 200 cycles, both the LiTFPFB and $LiBF_4$ electrolytes based cells exhibit slightly overpotential change compared with the 5^{th} cycle. Moreover, the $LiBF_4$ based battery shows a larger capacity fading (Figure S9b) and lower peak current than those of LiTFPFB (Figure S9a and Figure S9c) after 200 cycles.

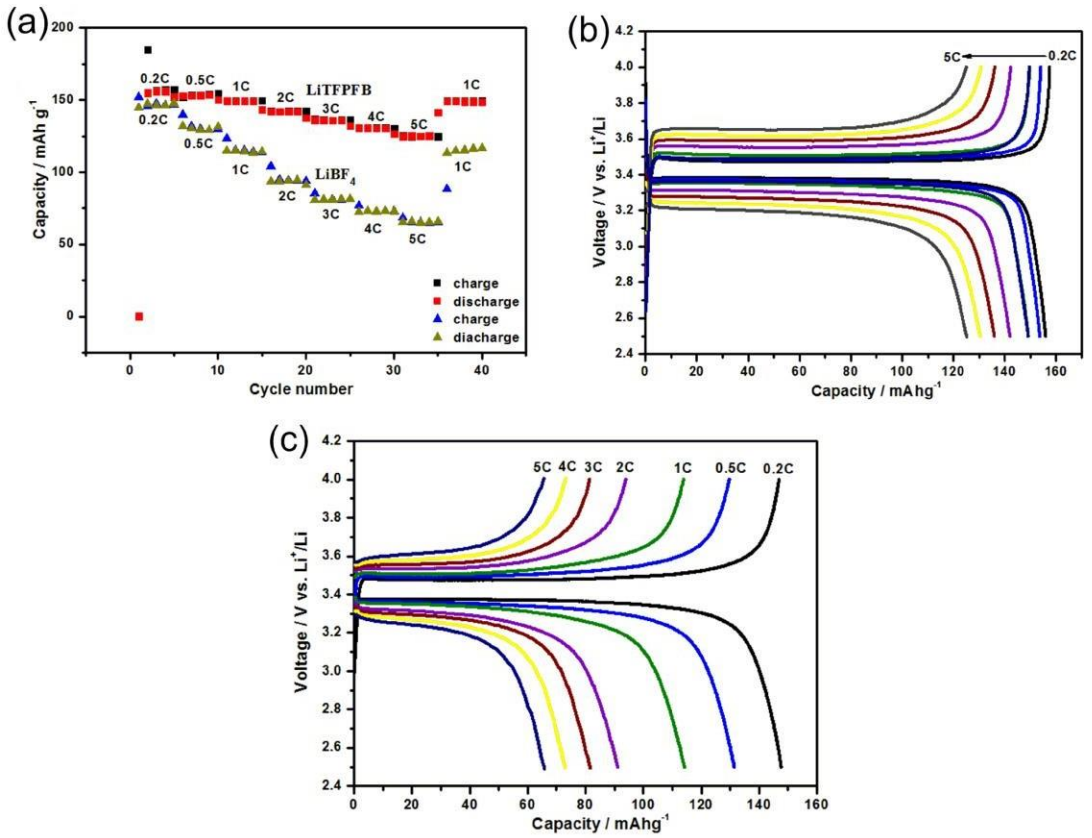

Figure S10. (a) Rate performance of $LiFePO_4$/Li cells with 1.0 M $LiBF_4$ and 1.0 M LiTFPFB electrolytes at room temperature. (b) The charge/discharge curves of LiTFPFB based $LiFePO_4$/Li cells at different rates. (c) The charge/discharge curves of $LiBF_4$ based $LiFePO_4$/Li cells at different rates.

Figure S10a exhibits the rate performance of LiTFPFB and $LiBF_4$ based batteries, wherein the charge/discharge current densities varied from 0.2 C to 5 C. Though the LiTFPFB based battery could not operate at the first cycle at 0.2 C (which might because the electrolyte cannot wet the separator and electrode initially), the rate capability of LiTFPFB based battery is much better than that of the $LiBF_4$ based battery. Furthermore, the LiTFPFB based battery exhibits typical flat-shaped plateau with relatively lower capacity fade (seen in Figure S10b)

compared with $LiBF_4$ based battery (Figure S10c), indicating the fast kinetics of lithium ion transport in the LiTFPFB based electrolyte. The excellent rate performance demonstrates that LiTFPFB possesses outstanding electrochemical stability and Li^+ conduction ability. This result can be attributed to the super-delocalized nature of the anion in LiTFPFB, which could improve the lithium ion dissociation and increase the number of free Li^+ compared with $LiBF_4$.

2.6 Impedance variation of the $LiFePO_4$/Li cells using different electrolytes

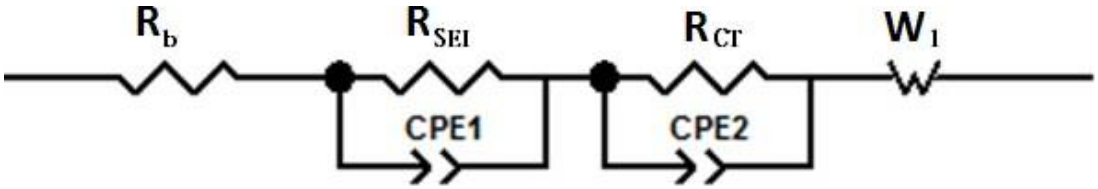

Figure S11.The equivalent circuit of the AC-impedance plots.

Table S1. The fitted R_b, R_{SEI} and R_{CT} results of the $LiFePO_4$/Li cells

Electrolyte	1.0 M LiTFPFB in PC			1.0 M $LiBF_4$ in PC		
Resistance	R_b (Ω)	R_{SEI} (Ω)	R_{CT} (Ω)	R_b (Ω)	R_{SEI} (Ω)	R_{CT} (Ω)
1st cycle	2.6	3.0	10.0	10.4	13.1	11.0
50th cycle	2.3	3.4	11.8	13.0	26.0	9.0
100th cycle	5.4	6.5	7.6	6.3	31.8	7.9
200th cycle	3.8	8.5	8.6	7.1	41.8	38.4

2.7 Low temperature performances of both electrolytes

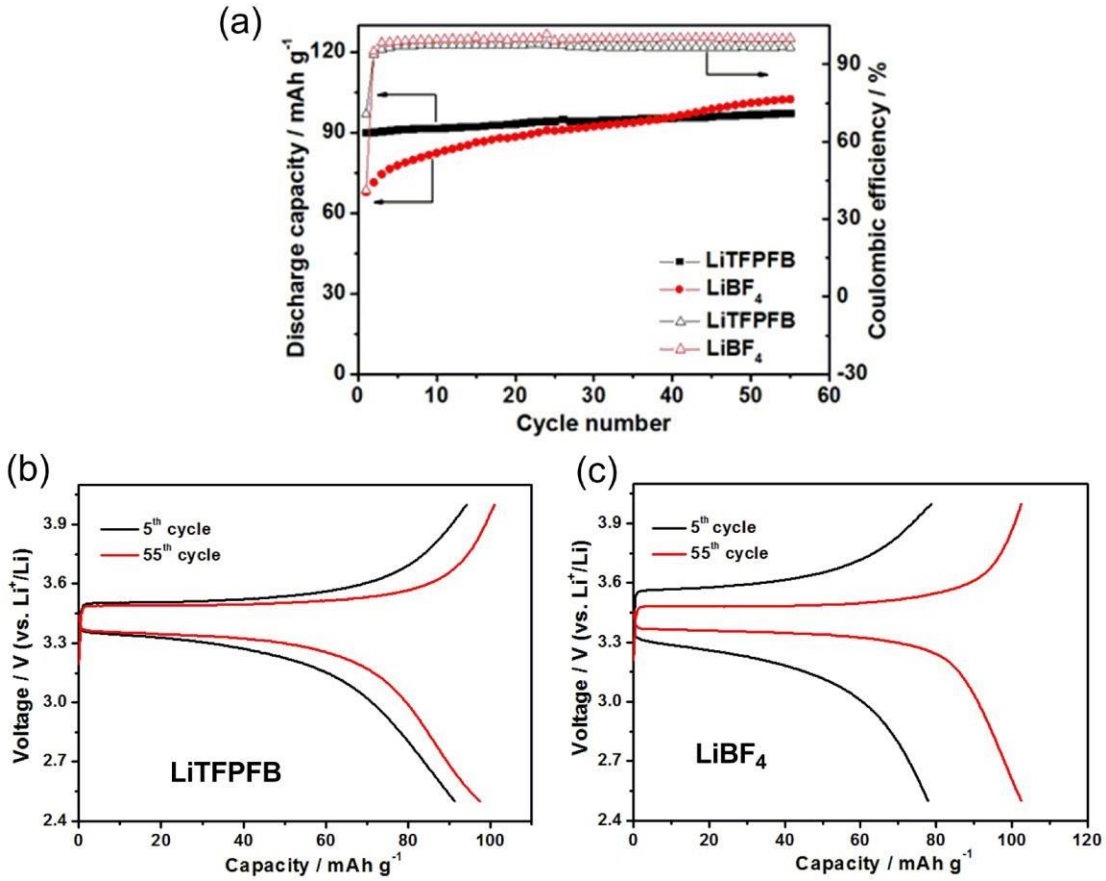

Figure S12. (a) Cycling performance of the $LiFePO_4$/Li metal cells using 1.0 M LiTFPFB/PC and 1.0 M $LiBF_4$/PC electrolytes with a current rate of 0.2 C at -5 °C. (b, c) The 5^{th} and 55^{th} charge-discharge profiles of the cells using LiTFPFB/PC and 1.0 M $LiBF_4$/PC electrolytes, respectively.

As shown in Figure S12a, the $LiFePO_4$/Li cell delivers an initial discharge capacity of 90.2 mAh g^{-1} at 0.2 C at -5 ℃ and the corresponding initial Coulombic efficiency is 70.6%, both of which are much higher than those of $LiBF_4$ based cell (67.9 mAh g^{-1} and 41.1%, respectively). The 5^{th} charge-discharge curve for LiTFPFB based cell is plotted in Figure S12b, which shows improved charge-discharge capacity

as well as lower overpotential compared with that of $LiBF_4$ based one (Figure S12c). It is noted from Figure S12 that the cell using LiTFPFB based electrolyte also exhibits a gradually improved cycling performance, while the $LiBF_4$ based cell shows a lower discharge capacity until 40 cycles, although a sharp growth trend is observed. Furthermore, from 41 to 55 cycles, the $LiBF_4$ based cell displays a gradually improved capacity than that of LiTFPFB, which is possibly due to self-conditioning of $LiBF_4$/PC electrolyte and slow penetration of the electrolyte into the cathode at low temperature. At the 55^{th} cycle (Figure S12b,c), the discharge capacity of the $LiBF_4$ based cell is 105.2 mAh g^{-1} and the Coulombic efficiency is 100%, which is slightly higher than that of LiTFPFB (97.4 mAh g^{-1} and 97.5%, respectively).

2.8 Summary of atomic surface concentrations

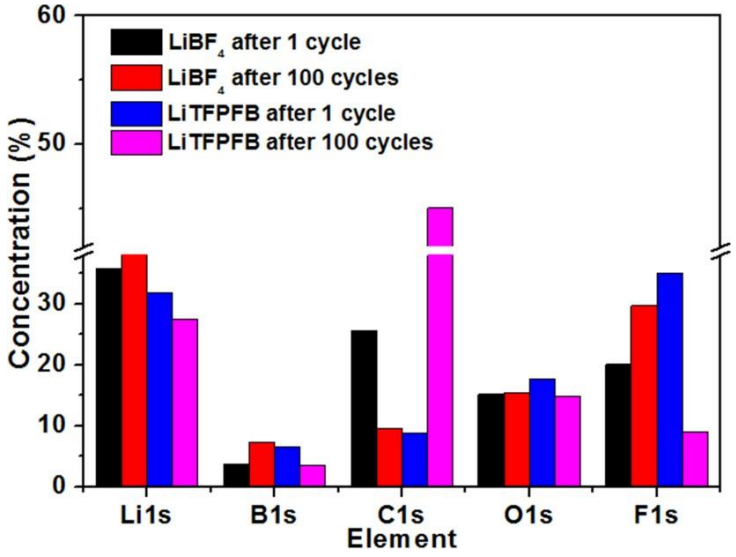

Figure S13. Surface atomic concentration obtained from XPS survey scans of Li anode in $LiFePO_4$/Li cells using 1.0 M $LiBF_4$ and 1.0 M LiTFPFB based electrolytes after 1 and 100 cycles at 60 °C.

Table S2. Summary of atomic surface concentration obtained from XPS survey scans

		Element concentration (%)				
		Li	B	C	O	F
1 M $LiBF_4$ in	After 1 cycle	35.8	3.7	25.6	15.2	20.1
PC solvent	After 100 cycles	38.1	7.3	9.5	15.4	29.7
1 M LiTFPFB	After 1 cycle	31.9	6.6	8.8	17.7	35.1
in PC solvent	After 100 cycles	27.6	3.5	45.0	14.9	9.0

Figure S13 and Table S2 show the XPS data collected for the Li anodes.

Analysis of the collected data reveals slight differences in the concentration of reacted species on the anode surface. Particularly, the dramatic concentration increase of C species and sharp decrease of F species might verify the decomposition of TFPFB anion.